Electronic Supplementary Material (ESI) for Chemical Communications.

Supplementary Information

Peptide Nanotubes Self-Assembled from Leucine-Rich Alpha Helical Surfactant-Like Peptides

Valeria Castelletto,[Ⓢ] Jani Seitsonen,[#] Janne Ruokolainen[#] Cristian Piras,[Ⓢ] Rainer Cramer,[Ⓢ] Charlotte J. C. Edwards-Gayle, [⚐] and Ian W. Hamley[Ⓢ,*]

[Ⓢ]Department of Chemistry, University of Reading. Reading RG6 6AD, United Kingdom.

[#]Nanomicroscopy Center, Aalto University, Puumiehenkuja 2, FIN-02150 Espoo, Finland.

[⚐]Diamond Light Source, Harwell Science and Innovation Campus, Fermi Avenue, Didcot OX11 0DE, United Kingdom

* Authors for correspondence

Experimental

Materials. Peptide R_3L_{12} was supplied by Peptide Protein Research Ltd. (Fareham, United Kingdom). The purity was > 95% by HPLC using an acetonitrile (0.1% TFA)/water (0.1% TFA) gradient. The molar mass by ESI-MS was 1885.525 $gmol^{-1}$. Scheme S1 shows the molecular structure of R_3L_{12}.

Sample Preparation. A stock solution of peptide was prepared by dissolving the peptide at 10 (22) wt% in hexafluoroisopropanol (HFIP), because R_3L_{12} is a highly hydrophobic peptide. An aliquot 1 µl of 12 (22) wt% R_3L_{12} in HFIP was added to 15 µl of MilliQ water inside a 1.5 ml Eppendorf. The Eppendorf was then vigorously vortexed while adding 2×145 µl of MilliQ water, 10 mM HCl or 100 mM HCl to obtain 0.04 (0.07) wt% R_3L_{12} at pH 4 (native), 2 or 1 respectively.

Liquid AP-MALDI MS.[1] α-cyano-4-hydroxycinnamic acid (CHCA) was used as the MALDI matrix chromophore. Briefly, 30 mg/ml CHCA was dissolved in acetonitrile/water (70:30; v:v) by sonication for 2 minutes, this solution was subsequently diluted 10:7 (v:v) with ethylene glycol, resulting in the liquid support matrix (LSM).[2] Immediately before MS analysis, 0.7 µl of analyte solution was mixed with 0.7 µl of LSM directly on the MALDI sample plate. All samples were analysed on a Synapt G2-Si instrument (Waters Corporation, Wilmslow, UK) equipped with a modified AP-MALDI source as previously described,[3] using MassLynx 4.1 software (Waters Corporation).

Circular Dichroism (CD) Spectroscopy. CD spectra were recorded using a Chirascan spectropolarimeter (Applied Photophysics, UK). Peptide solutions were placed in a quartz bottle (1 mm path length). Spectra were measured with a 0.5 nm step, 1 nm bandwidth, and 1 s collection time per step. The CD signal from the water background was subtracted from the CD data of the sample solutions.

Ellipticity is reported as the mean residue ellipticity ([θ], in deg cm^2 $dmol^{-1}$) and calculated as:

$$[\theta] = [\theta]_{obs}\, MRW(10\, c\, l)^{-1} \qquad \text{(S1)}$$

$[\theta]_{obs}$ is the ellipticity measured in millidegrees, MRW is the mean residue molecular weight of the peptide (molecular weight divided by the number of amino acid residues = 15, Scheme S1), c is the total concentration in mg/ml, and l is the optical path length of the cell in cm.

CD spectra were dominated by an α-helical secondary structure. The α-helix content, f_α, is calculated as:[4]

$$f_\alpha = 100\, [\theta]_{222}/[\theta]_{222,ex} \qquad \text{(S2)}$$

$[\theta]_{222,ex}$ in Equation S2 is the extrapolated value for the molar ellipticity:

$$[\theta]_{222,ex} = [\theta]^{\infty}(1 - k/n) \qquad \text{(S3)}$$

Here $[\theta]_{222,ex}$= -29608 deg cm^2 $dmol^{-1}$ because $[\theta]^{\infty}$ = -37400 deg cm^2 $dmol^{-1}$ is the maximum mean residue ellipticity at 222 nm of a peptide with infinite length and 100% helix content,[4] n= 12 is the number of residues/helix (L- residues; Scheme S1) and k is a wavelength-dependent constant (2.5 at 222 nm).

Cryogenic-Transmission Electron Microscopy (Cryo-TEM). Imaging was carried out using a field emission cryo-electron microscope (JEOL JEM-3200FSC), operating at 200 kV. Images were taken in bright field mode and using zero loss energy filtering (omega type) with a slit width of 20 eV. Micrographs were recorded using a Gatan Ultrascan 4000 CCD camera. The specimen temperature was maintained at -187 °C during the imaging. Vitrified specimens were prepared using an automated FEI Vitrobot device using Quantifoil 3.5/1 holey carbon copper grids with a hole size of 3.5 μm. Just prior to use, grids were plasma cleaned using a Gatan Solarus 9500 plasma cleaner and then transferred into the environmental chamber of a FEI Vitrobot at room temperature and 100 % humidity. Thereafter 3 μl of sample solution was applied on the grid and it was blotted twice for 5 seconds and then vitrified in a 1/1 mixture of

liquid ethane and propane at temperature of -180 °C. The grids with vitrified sample solution were maintained at liquid nitrogen temperature and then cryo-transferred to the microscope.

The thickness of the nanotubes and the thickness of the nanotube walls were measured from the cryo-TEM images using imageJ software.

Small-Angle X-Ray Scattering (SAXS). Synchrotron SAXS experiments on solutions were performed using a BioSAXS robots on beamline B21 (Diamond Light Source Ltd., UK). Solutions were loaded into the 96 well plate of an EMBL BioSAXS robot, and then injected via an automated sample exchanger into a quartz capillary (1.8 mm internal diameter) in the X-ray beam. The quartz capillary was enclosed in a vacuum chamber, in order to avoid air scattering. After the sample was injected in the capillary and reached the X-ray beam, the flow was stopped during the SAXS data acquisition. B21 operated with a fixed camera length (3.9 m) and fixed energy (12.4 keV). The images were captured using a Pilatus 2M detector. Data processing (background subtraction, radial averaging) was performed using the dedicated beamline software ScÅtter.

SAXS models. The SAXS curves in were fitted using an analytical expression for a form factor describing the convolution of cylindrical cylinders with a set of Gaussian functions to represent the electron density variation across the nanotube wall, with an electron dense core and less dense surfaces.[5-6]

The fitting parameters for the cylindrical shell form factor were the core radius, R, the shell thickness, D_r, and the scattering length density of the core, η_{core}, shell, η_{shell}, and solvent, η_{solv}.

The Gaussian membrane form factor was originally formulated for a Gaussian lipid bilayer membrane. The model assumes an electron density profile comprising Gaussian functions

for the head groups on either side of the membrane and another Gaussian for the hydrocarbon chain interior. The midpoint of the bilayer is defined as $z = 0 = z_C$.[7] The model assumes a Gaussian distribution of inter-head group thicknesses $2z_H$, with an associated Gaussian width Δ_{2zH}. The fitting parameters of the model are the electron densities of the head group, η_H, the layer thickness, $2z_H$, the electron density of the hydrocarbon chains, η_H, the standard deviation of the position of the Gaussian peak at z_H, σ_H, the standard deviation of the position of the Gaussian peak at z_C, σ_C, and Δ_{2zH}. All fitting was done using the software SASfit.[8]

Transmission Electron Microscopy (TEM). TEM imaging was performed using a JEOL 2100Plus TEM microscope operated at 200 kV. A drop of 0.04 wt% R_3L_{12} at pH 1 was placed on Cu grids coated with a carbon film (Agar Scientific, UK), stained with 1 wt% uranyl acetate acid (Sigma-Aldrich, UK) and dried.

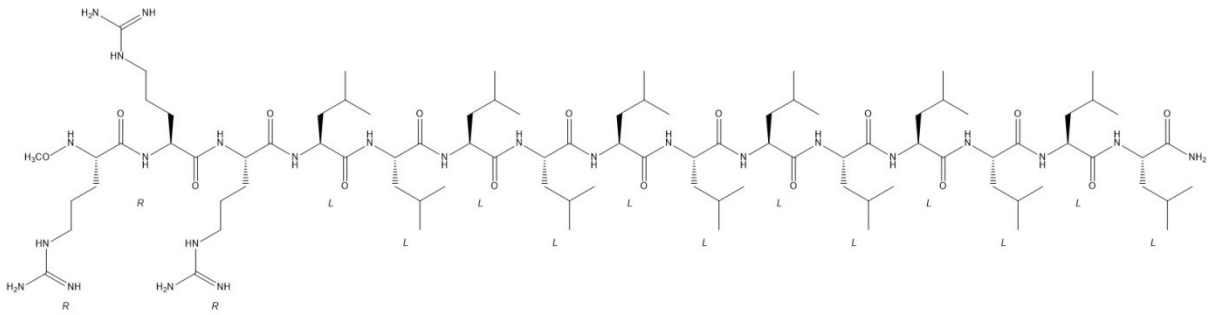

Scheme S1. Molecular structure of peptide R_3L_{12}, capped at both termini.

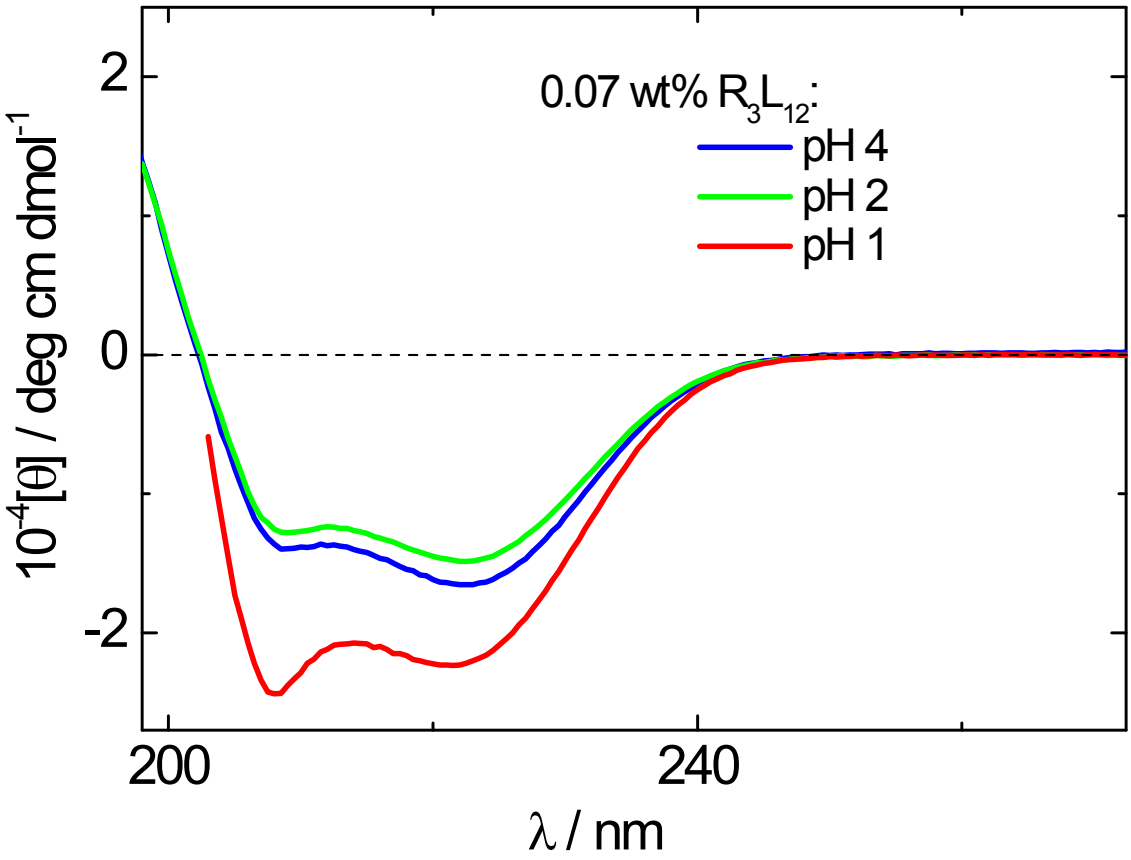

Figure S1. CD spectra measured for 0.07 wt% R_3L_{12} at pH 4 (native), 2 and 1.

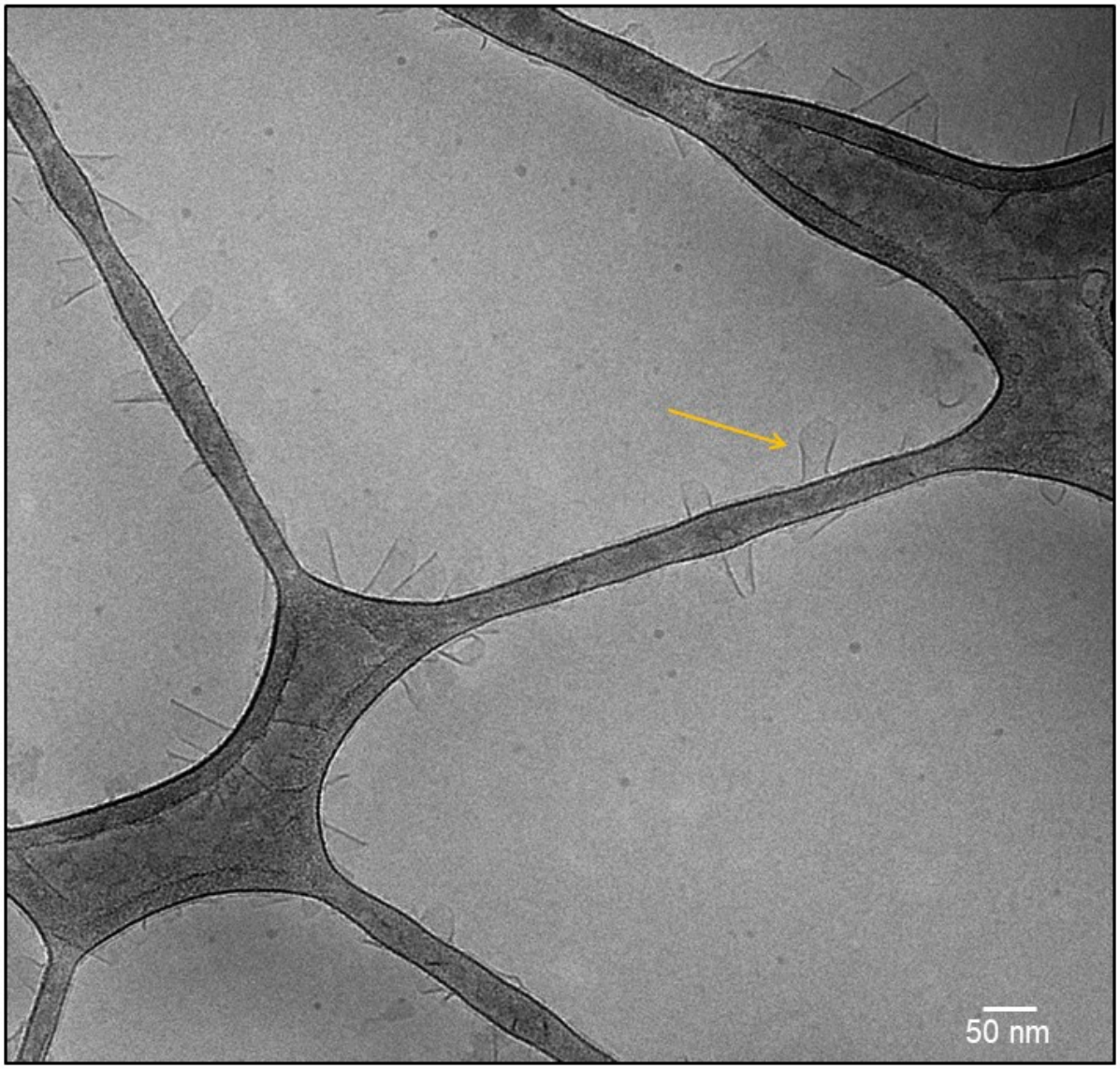

Figure S2. Cryo-TEM image for 0.04 wt% R_3L_{12} pH 4 (native). The orange arrow points to a representative nanotube.

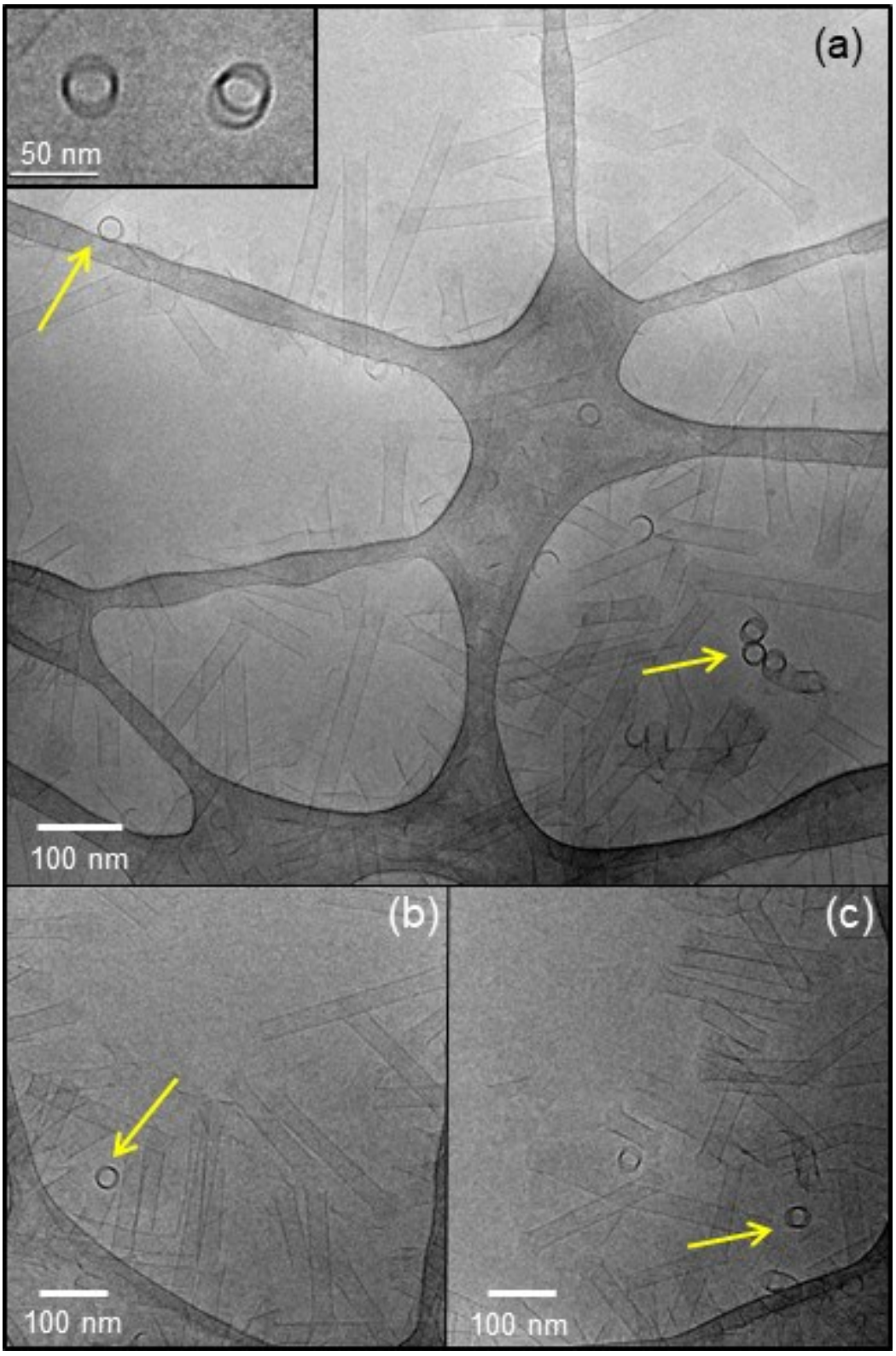

Figure S3. (a-c) Cryo-TEM images for 0.04 wt% R_3L_{12} at pH 2. The yellow arrows point to nanotube cross sections, similar to those magnified in the inset in (a).

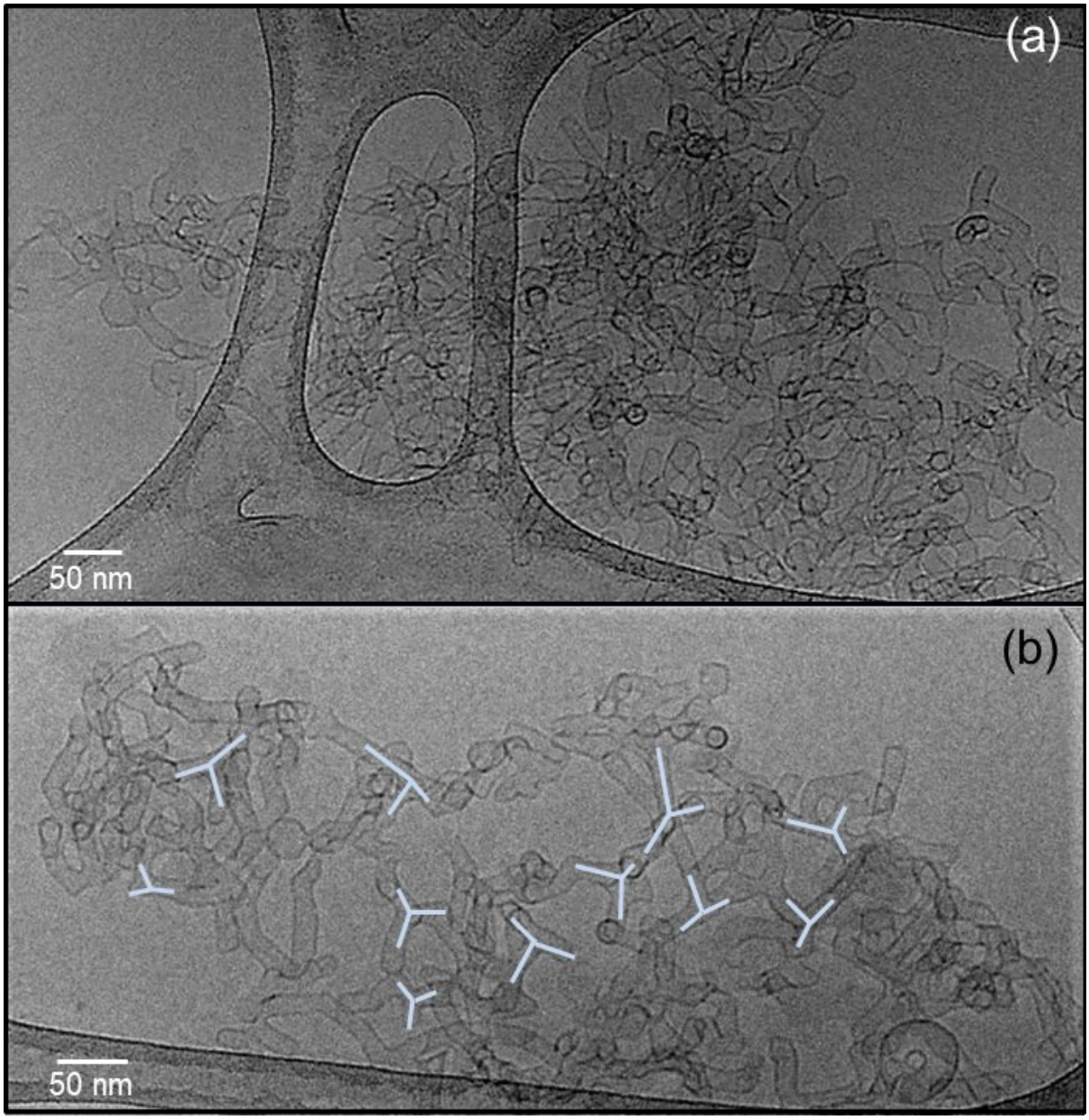

Figure S4. (a-b) Cryo-TEM images for 0.04 wt% R_3L_{12} at pH 1, showing nanotubes connected in bi-continuous networks. The blue tripods in (b) identify representative nanotube connections similar to that displayed in Scheme 1b.

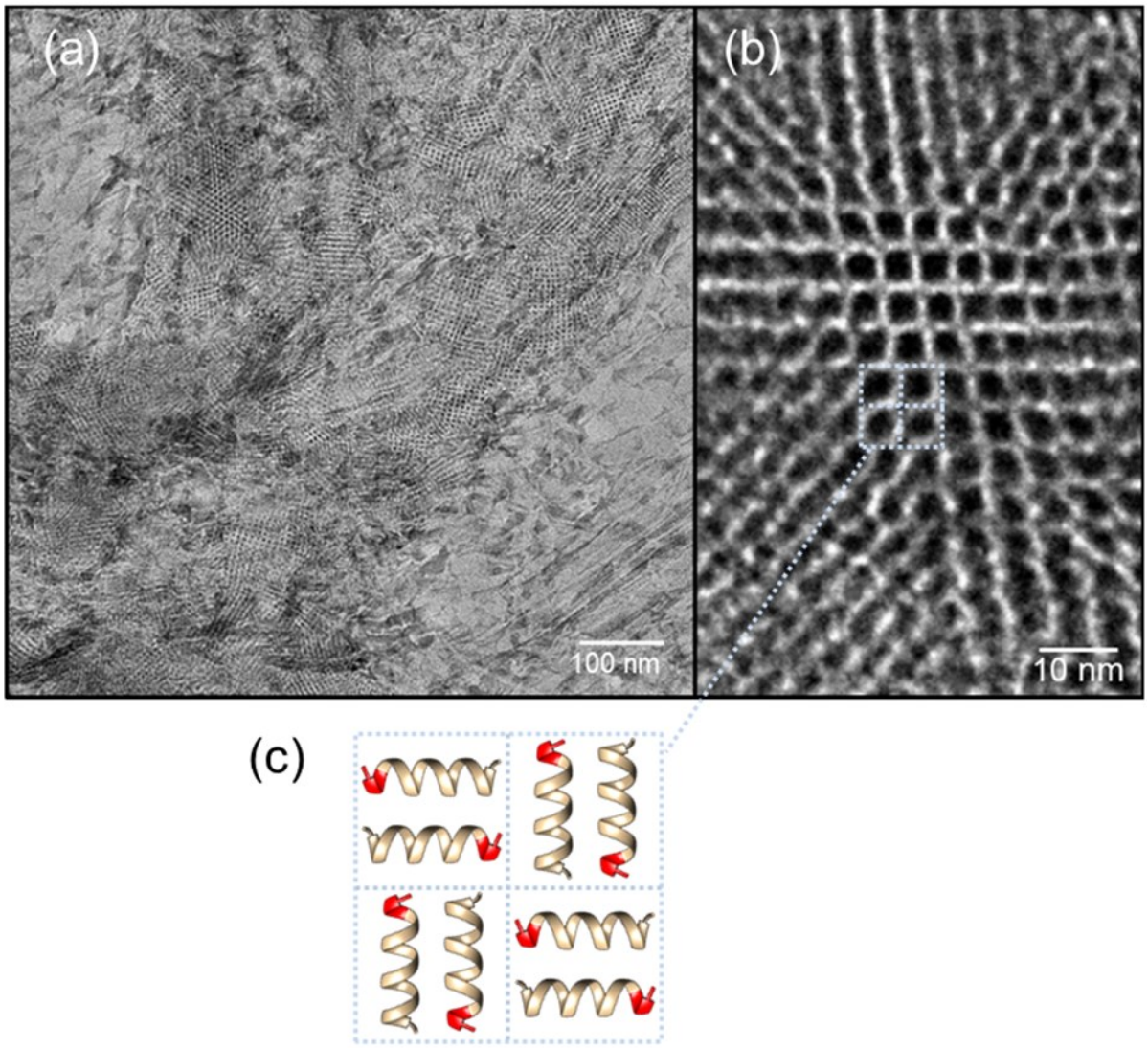

Figure S5. (a-b) TEM images for a film dried from a 0.04 wt%, pH 1, R_3L_{12} solution. (b) High resolution image of the squared pattern observed only for these dried films. Scheme (c) shows the orientation of the R_3L_{12} α-helices leading to the squared pattern observed in (a-b).

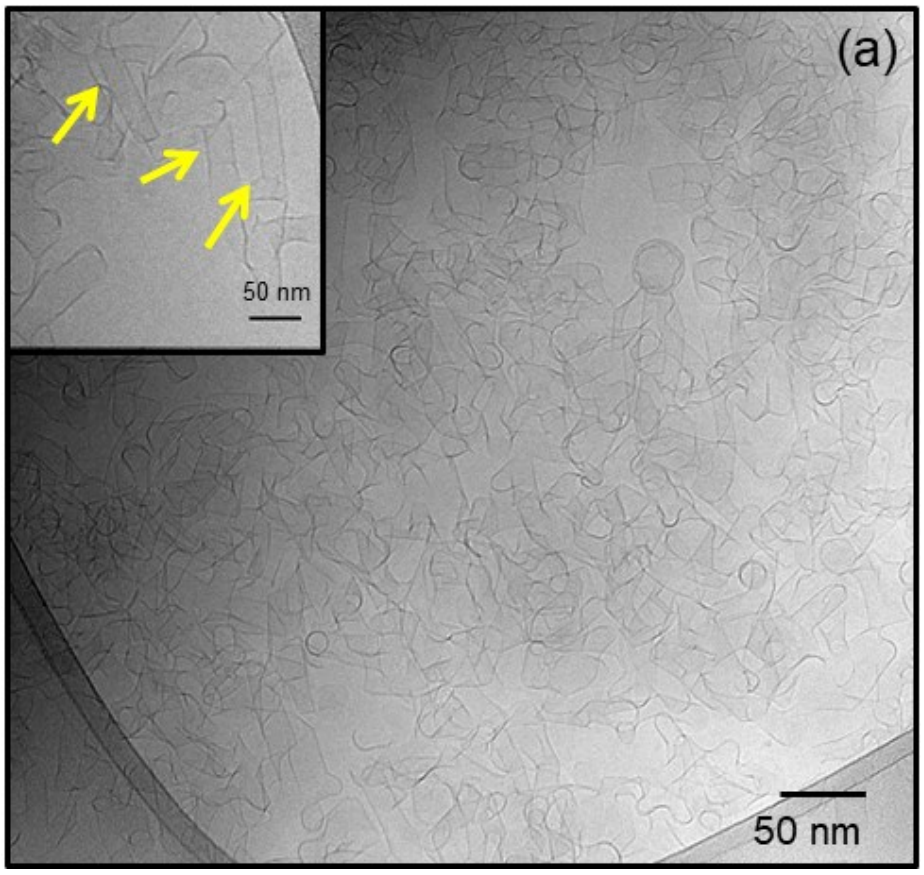

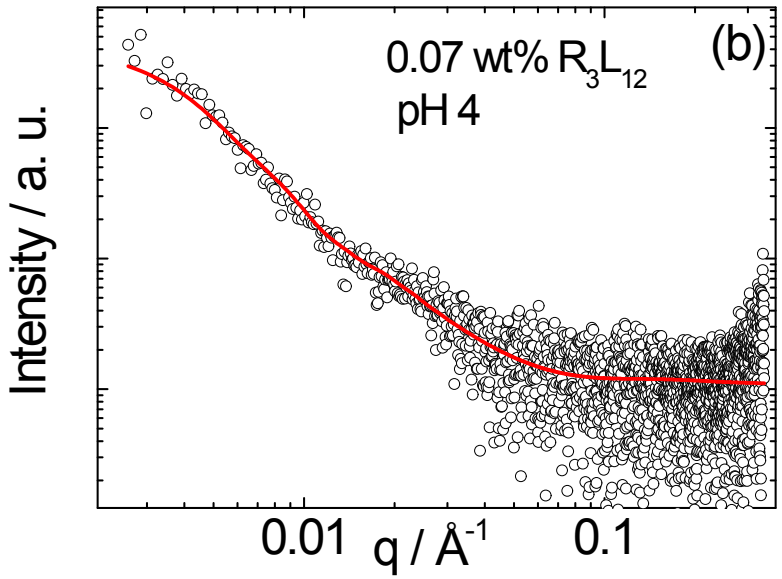

Figure S6. (a) Representative cryo-TEM images for 0.07 wt% acR_3L_{12} at pH 4 (native). Yellow arrows in the inset indicate some of the very few nanotubes observed in the images. (b) SAXS. The full in (b) is a fitting according to the model described in the text and the SI.

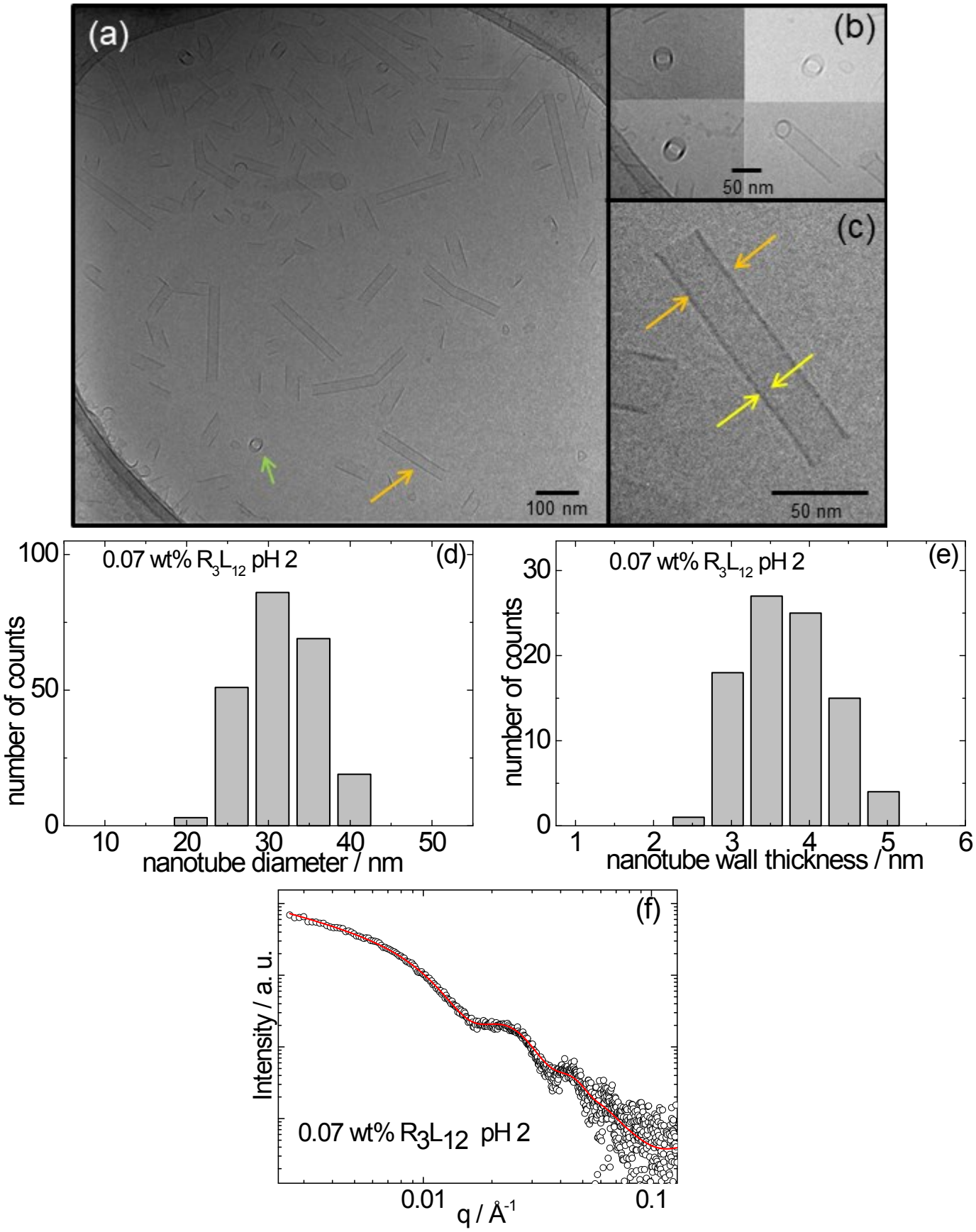

Figure S7. (a-c) Cryo-TEM images recorded for 0.07 wt% acR_3L_{12} at pH 2. (a) The orange arrow indicates a nanotube and the green arrow points to a nanotube cross section, similar to those in (b). Orange and yellow arrows in (c) indicate the thickness of a nanotube or a nanotube wall respectively. Histograms showing the (d) nanotube diameter or (e) the nanotube wall thickness measured from a series of cryo-TEM images. (f) SAXS data. The full line in (f) is a fitting according to the model described in the text and the SI.

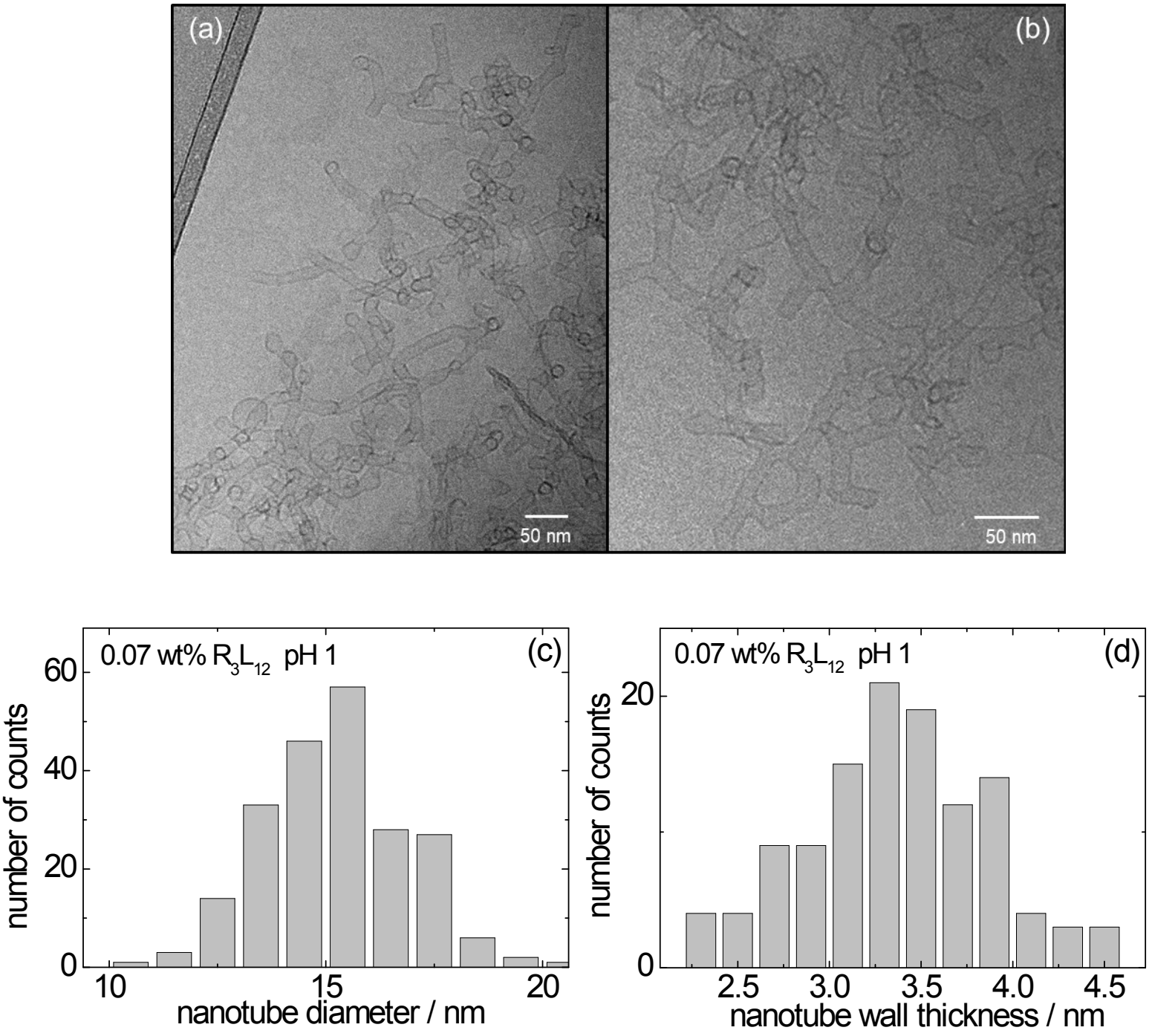

Figure S8. (a-c) Cryo-TEM images recorded for 0.07 wt% R_3L_{12} at pH 1. (a) The orange arrow indicates a nanotube and the green arrow points to a nanotube cross section, similar to those in (b). Orange and yellow arrows in (c) indicate the thickness of a nanotube or a nanotube wall respectively. Histograms showing the (d) nanotube diameter or (e) the nanotube wall thickness measured from a series of cryo-TEM images.

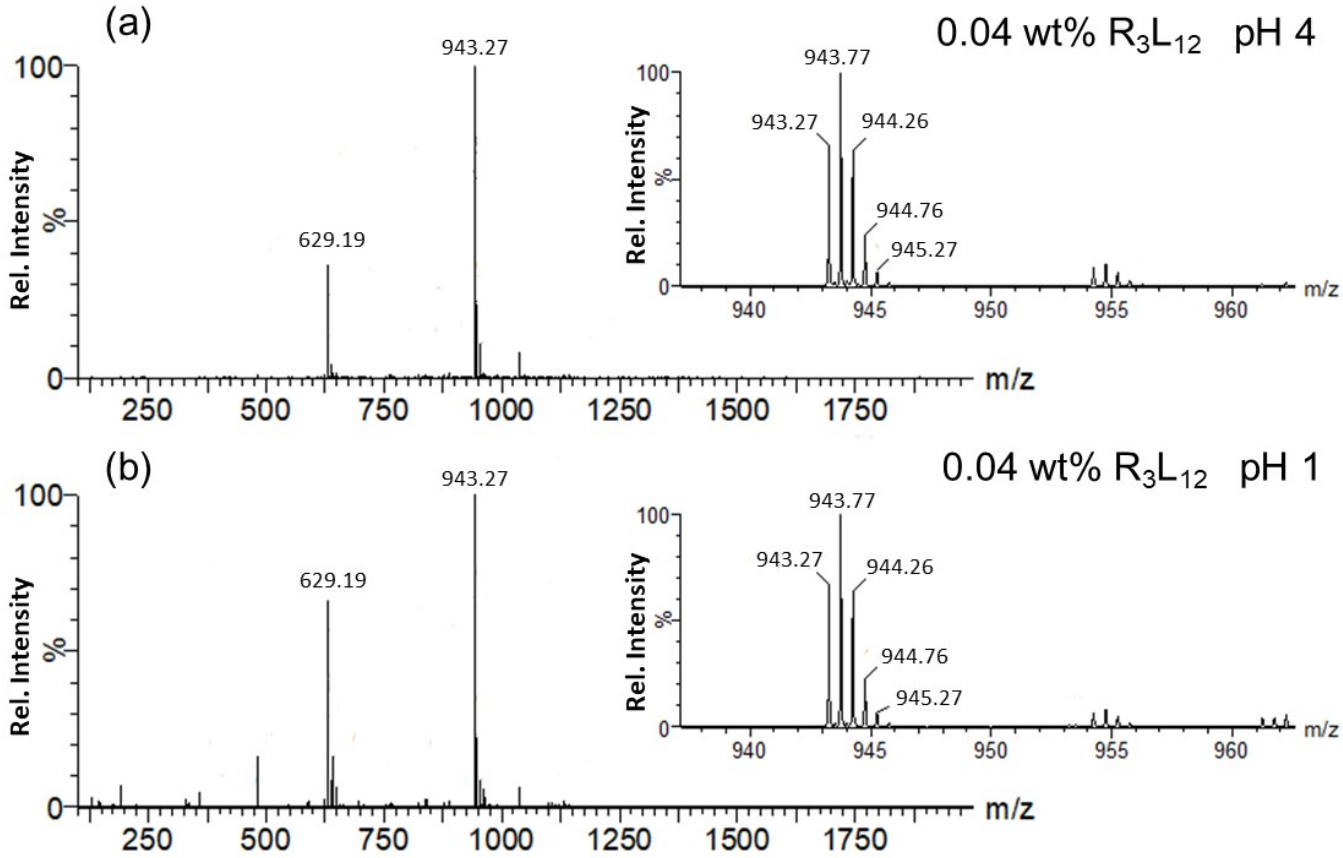

Figure S9. Liquid AP-MALDI MS spectra of 0.04 wt% R_3L_{12} at (a) pH 4 (native) and (b) pH 1. The insets in each panel magnify the m/z region of the $[M+2H]^{2+}$ ions. The ions detected in both liquid AP-MALDI MS spectra at m/z 629.19 and 943.27 represent the multiply charged peptide ion species $[M+3H]^{3+}$ and $[M+2H]^{2+}$ respectively, which are observed for both native pH and pH 1, indicating the absence of peptide degradation.

Table S1. Parameters extracted from the fitting of the SAXS in Figures 3, S6b and S7f, using the analytical models described in the 'SAXS models' section.

	0.04 wt% R_3L_{12} pH 4 (native)	0.07 wt% R_3L_{12} pH 4 (native)	0.04 wt% R_3L_{12} pH 2	0.07 wt% R_3L_{12} pH 2	0.04 wt% R_3L_{12} pH 1
N [a.u.]	0.05	0.009	0.013	0.001	0.008
R ± Δ R [Å]	158±17	120±60	130±15	135±20	62±20
D_r [Å]	25	30	35	25	30
η_{core} (a.u.)	$1.5x10^{-9}$	$1.5x10^{-9}$	$2.13x10^{-10}$	$1.49x10^{-9}$	$1.5x10^{-9}$
η_{shell} [a.u.]	$2.27x10^{-7}$	$2.3x10^{-7}$	$2.25x10^{-7}$	$3.27x10^{-7}$	$0.8x10^{-7}$
η_{solv} [a.u.]	$7.3x10^{-9}$	$7x10^{-9}$	$8.15x10^{-9}$	$7.08x10^{-9}$	$7.0x10^{-9}$
N_1 [a.u.]	0.9	0.09	0.5	1	0.06
$2z_H \pm \Delta_{2zH}$ [Å]	25 ± 10	25 ± 10	25 ± 10	25	25 ± 10
σ_H [Å]	3.8	2.5	2.5	3.75	2.5
η_H [rel. units]	$-2.25x10^{-7}$	$-1.0x10^{-7}$	$-1.3x10^{-7}$	$-1.86x10^{-7}$	$-2.1x10^{-7}$
σ_C [Å]	5	3	3	5	3
η_C [rel. units]	$8.94x10^{-8}$	$8.252x10^{-8}$	$8.25x10^{-8}$	$1.04x10^{-7}$	$8.252x10^{-8}$
BG	$1x10^{-4}$	$1.1x10^{-3}$	$1x10^{-4}$	$1x10^{-4}$	$1.2x10^{-3}$

Key. Cylindrical core-shell: scale factor, N, core radius, R, shell thickness, D_r, scattering length density of the core, η_{core}, shell, η_{shell}, and solvent, $\eta_{solv.}$ **Nanotube well Gaussian density profile form factor:** scale factor, N_1, Gaussian half-width at half-maximum for polydispersity, $\Delta_{2zH,}$ inter-head group thicknesses, $2z_H$, Gaussian half-width for outer layer surface, σ_H, electron density for headgroup, η_H, Gaussian half-width for inner layer, σ_C, relative electron density for inner layer, η_C. BG is the background.

Table S2. Structural parameters for R_3L_{13} α-helical nanotubes.

	*0.04 wt% R_3L_{12} pH 4 (native)	0.07 wt% R_3L_{12} pH 4 (native)	*0.04 wt% R_3L_{12} pH 2	*0.07 wt% R_3L_{12} pH 2	**0.04 wt% R_3L_{12} pH 1	**0.07 wt% R_3L_{12} pH 1
nanotube diameter: $2(R\pm\Delta R)+2D_r$ [nm]	36.6±3.4	30.0±12	33±3	32±4	18.0±4	--
nanotube diameter [nm]	32.5±6.3⑤	26.1±2.9	30.6±2.8⑤	31.7±4.5⑤	17.4±2.2⑤	15.2±1.6⑤
nanotube wall D_r [nm]	2.5	3	3.5	2.5	3	--
Wall thickness (Gaussian profile): $(2z_H\pm\Delta_{2zH})+2\sigma_H$ [nm]	3.3±0.1	3.0±0.1	3.0±0.1	3.3	3.0±0.1	--
nanotube wall thickness [nm]	3.4±0.5⑤	3.2±0.5	3.7±0.6⑤	3.7±0.5⑤	3.4±0.5⑤	3.4±0.5⑤

Key. Samples: ■ parameters extracted from SAXS fittings (Table S1); ■ parameters measured from cryo-TEM images; ⑤averaged from the corresponding cryo-TEM histograms in Figures 1g-h, S7d,e, S8c,d; *individual nanotubes; **continuous tubular network.

References

(1) Cramer, R.; Pirkl, A.; Hillenkamp, F.; Dreisewerd, K., Liquid AP-UV-MALDI Enables Stable Ion Yields of Multiply Charged Peptide and Protein Ions for Sensitive Analysis by Mass Spectrometry. *Angew. Chem., Int. Ed. Engl.* **2013,** *52*, 2364.

(2) Krenkel, H.; Hartmane, E.; Piras, C.; Brown, J.; Morris, M.; Cramer, R., Advancing Liquid Atmospheric Pressure Matrix-Assisted Laser Desorption/Ionization Mass Spectrometry Toward Ultrahigh-Throughput Analysis. *Anal. Chem.* **2020,** *92*, 2931.

(3) Ryumin, P.; Brown, J.; Morris, M.; Cramer, R., Investigation and optimization of parameters affecting the multiply charged ion yield in AP-MALDI MS. *Methods* **2016,** *104*, 11.
(4) Su, J. Y.; Hodges, R. S.; Kay, C. M., Effect of chain length on the formation and stability of synthetic α-helical coiled coils. *Biochemistry* **1994,** *33*, 15501.
(5) Hamley, I. W.; Dehsorkhi, A.; Castelletto, V.; Furzeland, S.; Atkins, D.; Seitsonen, J.; Ruokolainen, J., Reversible helical ribbon unwinding transition of a self-assembling peptide amphiphile. *Soft Matter* **2013,** *9*, 9290.
(6) Hamley , I. W.; Dehsorkhi, A.; Castelletto, V., Self-Assembled Arginine-Coated Peptide Nanosheets in Water. *Chem. Comm.* **2013,** *49*, 1850.
(7) Pabst, G.; Rappolt, M.; Amenitsch, H.; Laggner, P., Structural information from multilamellar liposomes at full hydration: Full q-range fitting with high quality x-ray data. *Phys. Rev. E* **2000,** *62*, 4000.
(8) Bressler, I.; Kohlbrecher, J.; Thünemann, A. F., SASfit: a tool for small-angle scattering data analysis using a library of analytical expressions. *J. Appl. Cryst.* **2015,** *48*, 1587.